DOI 10.1007/s11182-021-02191-y
Russian Physics Journal, Vol. 63, No. 9, January, 2021 (Russian Original No. 9, September, 2020)

PHYSICS OF MAGNETIC PHENOMENA

THEORETICAL STUDY OF THE FREQUENCY MULTIPLIER BASED ON IRREGULAR QUARTER-WAVELENGTH MICROSTRIP RESONATOR WITH THIN MAGNETIC FILM

B. A. Belyaev,[1,2] A. V. Izotov,[1,2] An. A. Leksikov,[1] P. N. Solovev,[1,2] V. V. Tyurnev[1]

UDC 537.87+517.958

The characteristics of a frequency doubler on a resonant microstrip structure with a thin magnetic film were studied theoretically. The electrodynamic calculation of the structure was performed within the quasi-static approximation. Nonlinear response of film magnetization was calculated taking into account the second-order terms in the Landau-Lifshitz equation. The frequency response of the microstrip resonator was calculated. It was shown that due to the use of the resonant circuit, high efficiency of the input signal energy conversion into the output signal at a doubled frequency was achieved. The optimal values of the magnitude and direction of an external static magnetic field, which ensure the maximum output power at a doubled frequency, were determined.

Keywords: microstrip resonator, thin magnetic film, frequency multiplication, nonlinear magnetization oscillations.

INTRODUCTION

Extensive research on microwave properties of ferromagnetic materials, which started after Vladimir Arkadiev experimentally discovered ferromagnetic resonance (FMR) [1], lead to the creation of numerous microwave-range ferrite devices. Operation of most such devices is based on using the so-called first-order effects caused by the linear relationship between high-frequency magnetization and external microwave magnetic field. However, at relatively large microwave field amplitudes, the ferromagnetic medium can manifest strongly pronounced nonlinear properties. Earlier discovered effects of signal detection [2], conversion [3], and frequency doubling [4] are associated with the second-order nonlinearity. These effects are quadratic to the microwave field amplitude, so they manifest only at sufficiently large fields, but it is on them that operation of many ferromagnetic microwave devices is based. Among such devices, one can name a frequency doubler that is a segment of a rectangular waveguide with a ferrite sample [4–6]. The study of devices showed that the power of a signal at a doubled frequency significantly depends on the sample shape: the maximum was observed for a tangentially magnetized ferrite plate, in which ellipticity of magnetization precession increased considerably compared to a spherical sample [7]. The efficiency of second-harmonic generation can be increased, if in order to excite magnetization oscillations a resonator is used, in which the amplitude of microwave oscillations is significantly higher at the same input signal power [8].

[1]Kirensky Institute of Physics of the Siberian Branch of the Russian Academy of Sciences – Division of Federal Research Center “Krasnoyarsk Scientific Center of the Siberian Branch of the Russian Academy of Sciences”, Krasnoyarsk, Russia, e-mail: belyaev@iph.krasn.ru; iztv@mail.ru; a.a.leksikov@gmail.com; psolovev@iph.krasn.ru; tyurnev@iph.krasn.ru; [2]Siberian Federal University, Krasnoyarsk, Russia. Translated from Izvestiya Vysshikh Uchebnykh Zavedenii, Fizika, No. 9, pp. 3–14, September, 2020. Original article submitted May 21, 2020.

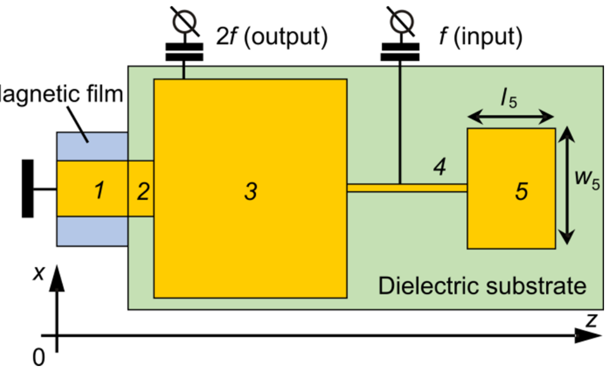

Fig. 1. Layout of the frequency multiplier on the microstrip resonator with a TMF.

Over the recent years, more and more publications have focused on nanocrystalline thin magnetic films (TMF) [9–13]. Saturation magnetization of such materials is several times higher than that of ferrites. That is why they have higher magnetic permeability in the microwave range. The most convenient way to excite oscillations in films is to use microstrip transmission lines (MTL). This ensures a higher coefficient of the planar structure filling with magnetic material and hence a more efficient interaction of magnetization with an electromagnetic wave. It is important to note that microstrip devices with TMF are easy to manufacture, rather compact, and compatible with integrated planar technology. A number of publications already demonstrated the feasibility of using nonlinear properties of TMF for frequency multiplication [14, 15] and conversion [16], as well as for parametric amplification of the input signal [17]. It is important that such research has not only scientific, but also significant applied value, as far as nonlinear devices based on magnetic materials can withstand considerably higher temperatures and radiation levels compared to devices based on semiconductor elements.

The present paper examines the model of a frequency doubler based on irregular quarter-wavelength microstrip resonator with a metallic TMF. The resonant design of the device allows for the efficient use of the input signal energy for the second harmonic generation. Multiplier characteristics are calculated within the quasi-static approximation. Nonlinear magnetization response was determined by solving the Landau-Lifshitz equation by method of successive approximations. The International System of Units is used in calculations.

1. MODEL OF MICROSTRIP FREQUENCY DOUBLER

The studied frequency doubler is built on the irregular quarter-wavelength microstrip resonator that consists of five cascade-connected segments of regular MTL (Fig. 1). Unlike the regular quarter-wavelength resonator, the irregular resonator used here has not the tripled, but the doubled resonant frequency of the second oscillation mode, and the resonant frequencies of its higher oscillation modes are not multiples of the first mode frequency, which considerably reduces the microwave power loss due to the higher harmonics. One end of the strip conductor of the resonator on segment *1* is grounded, forming the electric current (microwave magnetic field) antinode at all frequencies in this region of the resonator. That is why a metallic TMF deposited onto the glass substrate is placed here in contact with the ground plane. All other resonator segments are manufactured on the common dielectric substrate, and the end of the strip conductor on segment *5* remains open-circuited. The resonator is conductively connected to the input and output port via coupling capacities. Resonator tuning to resonant frequencies f_1 and $f_2 = 2f_1$ is done by selecting length l_i and width w_i of each of the resonator segments (i = 1–5).

A signal at frequency f is fed to the device. Its energy is non-uniformly distributed over all resonator segments. The energy stored up by the resonator on segment *1* ensures linear excitation of magnetization oscillations in TMF at frequency f. Nonlinear effects increase manifold in non-spherical samples due to the difference in demagnetization factors. That is why in such samples, the efficiency of microwave power conversion into oscillations at the doubled frequency is significantly higher. Second-order magnetization oscillations generate electromagnetic oscillations in the

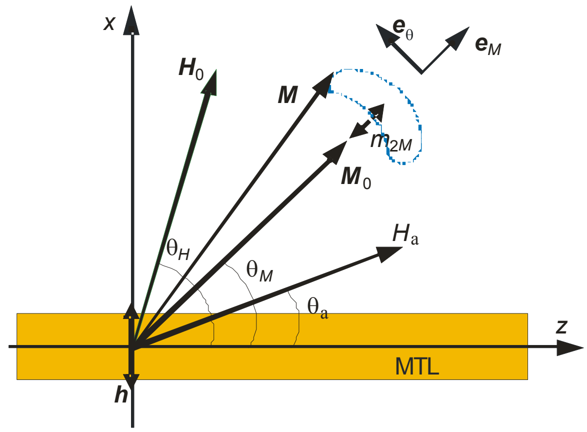

Fig. 2. Model of TMF with uniaxial magnetic anisotropy.

resonator at frequency $2f$, and their energy is fed to the device ports. Let us note that in a magnetic film, microwave energy absorption occurs along with multiplication of electromagnetic oscillation frequency, and this absorption is associated with ohmic and magnetic losses.

Let us turn to the derivation of formulas that allow calculating the main characteristics of the suggested multiplier model. For that, let us first consider the model of a single-domain TMF (Fig. 2) that is a nonlinear device element. The film has planar uniaxial magnetic anisotropy characterized by anisotropy field H_a and direction angle of easy magnetization axis (EMA) θ_a. Magnetic film is located between the substrate and the MTL ground plane. It is under static magnetic field $\boldsymbol{H}_0$ applied in the film plane and oriented at angle θ_H to axis z of the laboratory system of coordinates x, y, z. Microwave magnetic field $\boldsymbol{h}$ created by the current on the strip conductor is directed along axis x.

Energy density of film F that is the sum of Zeeman energy density, energy density of uniaxial magnetic anisotropy, as well as energy density of magnetic charges emerging on the film surfaces is expressed by formula

$$F = -\mu_0 \boldsymbol{MH} - \frac{\mu_0 H_a}{2M}(\boldsymbol{Mn})^2 + \frac{\mu_0}{2}\boldsymbol{M}\left(\overset{\leftrightarrow}{\boldsymbol{N}}\boldsymbol{M}\right). \tag{1}$$

Here $\boldsymbol{H} = \boldsymbol{H}_0 + \boldsymbol{h}$, $\boldsymbol{M} = \boldsymbol{M}_0 + \boldsymbol{m}$, $\boldsymbol{M}_0$ and $\boldsymbol{m}$ are the static and dynamic components of magnetization vector $\boldsymbol{M}$, $\boldsymbol{n}$ is the unit vector concurring with EMA direction, $\overset{\leftrightarrow}{\boldsymbol{N}}$ is the tensor of demagnetization factors, which in the case of a film sample has only one non-zero component $N_{yy} = 1$.

The motion of film magnetization $\boldsymbol{M}$ is described by the Landau-Lifshitz equation that has the following form:

$$\frac{\partial \boldsymbol{M}}{\partial t} = -\gamma \boldsymbol{M} \times \boldsymbol{H}^{\mathrm{eff}} + \frac{\alpha}{M}\boldsymbol{M} \times \frac{\partial \boldsymbol{M}}{\partial t}, \tag{2}$$

where $\gamma = 2.21 \cdot 10^5$ A^{-1}·s^{-1}·m is the gyromagnetic ratio, α is the dimensionless damping coefficient, M is the saturation magnetization of the film, $\boldsymbol{H}^{\mathrm{eff}} = -\mu_0^{-1} \partial F / \partial \boldsymbol{M}$ is the effective magnetic field. From condition of the energy density minimum F one can identify the direction angle of equilibrium magnetization θ_M [18]. It is the root of equation

$$H_0 \sin(\theta_H - \theta_M) + \frac{1}{2} H_a \sin 2(\theta_a - \theta_M) = 0. \tag{3}$$

Let us calculate the linear response of magnetization $\boldsymbol{m}_1$ to the microwave magnetic field $\boldsymbol{h}$ varying with time according to the law $\exp(-i\omega t)$. Solving in the linear approximation the equation of magnetization motion (2) in the local system of coordinates with unit vectors $\boldsymbol{e}_\theta$, $\boldsymbol{e}_y$, $\boldsymbol{e}_M$ that is associated with equilibrium magnetization $\boldsymbol{M}_0$, we find the complex amplitudes

$$
\begin{aligned}
m_{1\theta} &= \frac{\Omega_y \Omega_M}{\Omega_\theta \Omega_y - \omega^2} h_\theta - i \frac{\omega \Omega_M}{\Omega_\theta \Omega_y - \omega^2} h_y, \\
m_{1y} &= i \frac{\omega \Omega_M}{\Omega_\theta \Omega_y - \omega^2} h_\theta + \frac{\Omega_\theta \Omega_M}{\Omega_\theta \Omega_y - \omega^2} h_y, \\
m_{1M} &= 0,
\end{aligned}
\tag{4}
$$

where the following notations are introduced:

$$
\begin{aligned}
\Omega_\theta &= \gamma\big(H_0 \cos(\theta_H - \theta_M) + H_\mathrm{a} \cos 2(\theta_\mathrm{a} - \theta_M)\big) - i\omega\alpha, \\
\Omega_y &= \gamma\Big(H_0 \cos(\theta_H - \theta_M) + H_\mathrm{a} \cos^2(\theta_\mathrm{a} - \theta_M) + M\Big) - i\omega\alpha, \\
\Omega_M &= \gamma M.
\end{aligned}
\tag{5}
$$

This solution can be written in the brief tensor form $\boldsymbol{m}_1 = \ddot{\chi}\boldsymbol{h}$, where magnetic susceptibility $\ddot{\chi}$ is the second-rank tensor. The tensor of relative microwave magnetic permeability $\ddot{\mu}/\mu_0$ is related to the tensor of magnetic susceptibility by a simple expression $\ddot{\mu}/\mu_0 = 1 + \ddot{\chi}$. Hence the non-zero tensor components $\ddot{\mu}/\mu_0$ in the local system of coordinates are expressed by formulas

$$
\begin{aligned}
&\mu_{\theta\theta} = 1 + \frac{\Omega_y \Omega_M}{\Omega_\theta \Omega_y - \omega^2}, \quad \mu_{\theta y} = -i \frac{\omega \Omega_M}{\Omega_\theta \Omega_y - \omega^2}, \\
&\mu_{y\theta} = -\mu_{\theta y}, \quad \mu_{yy} = 1 + \frac{\Omega_\theta \Omega_M}{\Omega_\theta \Omega_y - \omega^2}, \quad \mu_{MM} = 1.
\end{aligned}
\tag{6}
$$

Propagation and nonlinear interaction of fundamental modes in MTL containing a ferromagnetic film will be described in the quasi-static approximation using telegraph equations. For that, one needs to calculate beforehand the electrical capacity per unit length C and inductance per unit length L of the MTL strip conductor with a magnetic film on segment *1*. Linear parameters of MTL will be calculated within the Oliner model [19], in which an equivalent flat waveguide is considered for the approximate calculation of line parameters instead of MTL itself. Fig. 3 shows the cross-section of MTL with a thin magnetic film of thickness t_f that was deposited onto the glass substrate with thickness t_g and permittivity ε_g. In this figure, semi-transparent shading indicates the section of the equivalent flat waveguide. From above and from below the waveguide is restricted along its entire width with ideal flat conductors. On the right and on the left, it has ideal vertical magnetic walls preventing the exit of microwave power outside its limits.

Permittivity of the filling of such a waveguide is considered equal to the effective permittivity of the microstrip line ε_e. Effective width w_e of the equivalent waveguide is selected such that its characteristic impedance Z_{WG} expressed by formula

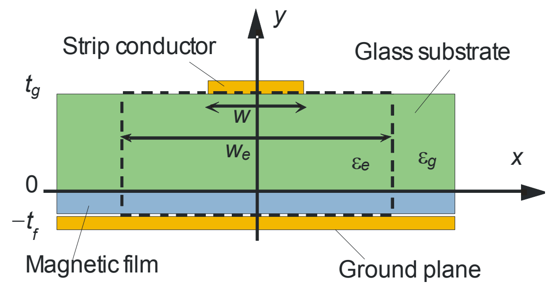

Fig. 3. Oliner model for a microstrip line (cross-section).

$$Z_{\mathrm{WG}} = \sqrt{\frac{\mu_0}{\varepsilon_0 \varepsilon_e}} \frac{t_g}{w_e}, \tag{7}$$

would equal the impedance of the microstrip line Z_{MS} for the case, when magnetic film is an ideal conductor. Utilities from software packages for the design of microstrip circuits or individual specialized software can be used to find values of effective parameters ε_e and Z_{WG} at given values of ε_g and strip conductor width w.

In an equivalent waveguide, we shall consider only the fundamental mode. This mode is strictly transversal at ideal magnetic film conductivity. Its electric field $\boldsymbol{E}$ and magnetic field $\boldsymbol{h}$ do not depend on coordinates x, y. At finite film conductivity, a fundamental mode becomes quasi-transversal. Due to the skin effect, its fields $\boldsymbol{E}$ and $\boldsymbol{h}$ strongly depend on the coordinate y inside the film. Meanwhile, field $\boldsymbol{E}$ inside the magnetic film is much smaller than in the glass substrate due to the high film conductivity. One can show that capacity per unit length of the equivalent waveguide conductors

$$C = \varepsilon_0 \varepsilon_e \, w_e / t_g \,. \tag{8}$$

Here ε_0 is the permittivity of vacuum. In the quasi-static approximation, parameters C, ε_e and w_e do not depend on the frequency and magnetic film parameters.

Magnetic field $\boldsymbol{h}$, unlike electric field $\boldsymbol{E}$, penetrates the metallic film, where it diminishes according to the exponential law of the skin effect. Let us calculate the quasi-static field oscillations $\boldsymbol{h}$ in MTL that are uniform along axis x. Let us start from calculating the field in the glass substrate, i.e. at $0 \le y \le t_g$. It is described by magnetostatics equations $\mathrm{rot}\,\boldsymbol{h} = 0$, $\mathrm{div}\,\boldsymbol{h} = 0$. Their solution, taking into account the boundary condition on the strip conductor surface with current I_1, is expressed by formulas

$$h_x = I_1 / w_e \,, \; b_y = 0, \; h_z = 0 \,. \tag{9}$$

Field $\boldsymbol{h}$ inside the magnetic film, i.e. at $-t_f \le y \le 0$, is described by Maxwell's equations, which after neglecting displacement currents $\partial\boldsymbol{D}/\partial t$ compared to conductivity currents $\sigma\boldsymbol{E}$ assume the form

$$\mathrm{rot}\,\boldsymbol{E} = i\omega\boldsymbol{b}, \quad \mathrm{rot}\,\boldsymbol{h} = \sigma\boldsymbol{E} \,, \tag{10}$$

where $\boldsymbol{b}$ is the magnetic induction vector, σ is the electrical conductivity of TMF. Then, neglecting derivatives $\partial/\partial z$ compared to derivatives $\partial/\partial y$ that differ by orders of magnitude due to the skin effect in electroconductive medium, and moving on to the field components in the local system of coordinates, we shall get equations

$$\partial^2 h_\theta / \partial y^2 = -i\omega\sigma b_\theta,$$

$$0 = -i\omega\sigma b_y, \tag{11}$$

$$\partial^2 h_M / \partial y^2 = -i\omega\sigma b_M.$$

Magnetic field strength and induction inside the film are related by equations

$$b_\theta = \mu_0 \left(\mu_{\theta\theta} h_\theta + \mu_{\theta y} h_y \right),$$

$$b_y = \mu_0 \left(\mu_{y\theta} h_\theta + \mu_{yy} h_y \right), \tag{12}$$

$$b_M = \mu_0 h_M.$$

Let us require that the normal component of induction on the upper and lower surface of the film satisfy the boundary condition $b_y = 0$. Then from formulas (12) we shall get

$$h_y = -h_\theta \, \mu_{y\theta} / \mu_{yy}. \tag{13}$$

In the local system of coordinates, the system of equations (11) taking into account formulas (12), (13) and continuity of component h_x on the film surface bordering on the glass substrate has the solution

$$h_\theta = \frac{I_1}{w_e} \frac{\cos\left(k_\theta (y + t_f)\right)}{\cos\left(k_\theta t_f\right)} \cos\theta_M,$$

$$h_y = -\frac{\mu_{y\theta}}{\mu_{yy}} \frac{I_1}{w_e} \frac{\cos\left(k_\theta (y + t_f)\right)}{\cos\left(k_\theta t_f\right)} \cos\theta_M, \tag{14}$$

$$h_M = \frac{I_1}{w_e} \frac{\cos\left(k_M (y + t_f)\right)}{\cos\left(k_M t_f\right)} \sin\theta_M.$$

Here the following notations are used:

$$k_M^2 = i\omega\sigma\mu_0, \quad k_\theta^2 = k_M^2 \mu_\theta, \quad \mu_\theta = \mu_{\theta\theta} + \mu_{y\theta}^2 / \mu_{yy}. \tag{15}$$

Value μ_θ is the effective permeability for the plane transverse wave propagating in the infinite medium perpendicularly to the equilibrium magnetization vector. It determines phase velocity and characteristic impedance of such a wave. Value μ_θ is also called transversal permeability [20].

To calculate inductance per unit length L on segment *1* (see Fig. 1) containing TMF, one needs to find the x-component of induction $\boldsymbol{b}(y)$. When calculating it, we shall neglect the nonlinear response of film magnetization. Substituting expressions (14) into formula (12) and using equation $b_x = b_\theta \cos\theta_M + b_M \sin\theta_M$, we shall get

$$b_x = \mu_0 \frac{I_1}{w_e}\left[\mu_\theta \frac{\cos\left(k_\theta (y+t_f)\right)}{\cos\left(k_\theta t_f\right)}\cos^2\theta_M + \frac{\cos\left(k_M (y+t_f)\right)}{\cos\left(k_M t_f\right)}\sin^2\theta_M\right]. \tag{16}$$

In the glass substrate, induction $b_x(y)$, according to formula (9), equals $\mu_0 I_1 / w_e$.

Linear magnetic induction flux through the circuit of unit length encompassing the longitudinal section of MTL with thickness $t_f + t_g$ is determined by expression $\Psi(\omega) = \int_{-t_f}^{t_g} b_x(y)\, dy$. After integration, we shall use formula $L = \Psi/I_1$ to find inductance per unit length of MTL with a magnetic film

$$L(\omega) = \frac{\mu_0}{w_e}\left[t_g + t_f \mu_\theta(\omega)\frac{\mathrm{sinc}(k_\theta t_f)}{\cos(k_\theta t_f)}\cos^2\theta_M + t_f \frac{\mathrm{sinc}(k_M t_f)}{\cos(k_M t_f)}\sin^2\theta_M\right]. \tag{17}$$

Taking into account that inductance per conductor unit length of the flat waveguide on the glass substrate is expressed by formula $L = \mu_0 \mu_e t_g / w_e$, let us find the effective relative permeability of MTL

$$\mu_e(\omega) = 1 + \frac{t_f}{t_g}\mu_\theta(\omega)\frac{\mathrm{sinc}(k_\theta t_f)}{\cos(k_\theta t_f)}\cos^2\theta_M + \frac{t_f}{t_g}\frac{\mathrm{sinc}(k_M t_f)}{\cos(k_M t_f)}\sin^2\theta_M . \tag{18}$$

To find the distribution of current $I_1(z)$ and voltage $U_1(z)$ along the resonator length at frequency ω, let us turn to the system of telegraph equations

$$\partial U_1/\partial z + L(\omega)\partial I_1/\partial t = 0, \qquad \partial I_1/\partial z + C\,\partial U_1/\partial t = 0 . \tag{19}$$

Taking into account that the flat conductor is grounded in point $z = 0$, we shall find the solution to this system

$$I_1(z) = I_1 \cos\left(k_1 z\right), \qquad U_1(z) = iZ_1 I_1 \sin(k_1 z), \tag{20}$$

where wave vector k_1 and characteristic impedance Z_1, according to formulas (8) and (17), assume values

$$k_1 = \frac{\omega}{\tilde{n}}\sqrt{\varepsilon_e \mu_e(\omega)}, \quad Z_1 = Z_0 \sqrt{\mu_e(\omega)/\varepsilon_e}\,\frac{t_g}{w_e}. \tag{21}$$

Here c is the speed of light in the free space, $Z_0 = \sqrt{\mu_0/\varepsilon_0}$ is the characteristic impedance of free space. Therefore, we have produced the calculation formulas to determine the characteristics of MTL with a magnetic film taking into account only its linear response.

Let us now calculate the magnetization oscillations of the film $\boldsymbol{m}_2$ at frequency 2ω. Emergence of the harmonic $\boldsymbol{m}_2$ is associated with existence of the non-harmonic oscillation of the longitudinal component m_M, which is the consequence of constancy of the absolute value of vector $\boldsymbol{M}$ and inequation $|m_{1\theta}| \neq |m_{1y}|$ for the components of the linear response of magnetization $\boldsymbol{m}$ to field $\boldsymbol{h}$. Value m_M with an accuracy to quadratic terms in relation to the linear response components is expressed by formula

$$m_M = -\frac{1}{2M}\left(m_{1\theta}^2 + m_{1y}^2\right). \tag{22}$$

Let us calculate the linear magnetic induction flux Ψ generated by non-harmonic magnetization oscillation m_M at frequency 2ω via the longitudinal section of MTL between the strip conductor and the ground plane. As far as linear harmonic components $m_{1\theta}$ and m_{1y} are phase-shifted by $\pi/2$, the flux Ψ generated by it will oscillate between its extreme values

$$\Psi_\theta = -\frac{\mu_0 \sin\theta_M}{2M}\int_{-t_f}^{0} m_{1\theta}^2 dy, \quad \Psi_y = -\frac{\mu_0 \sin\theta_M}{2M}\int_{-t_f}^{0} m_{1y}^2 dy\,. \tag{23}$$

In this case, it was taken into account that projection m_M onto axis x equals $m_M \sin\theta_M$. One can see that induction flux Ψ is the sum of static displacement $\Psi_0 = -\left(|\Psi_\theta| + |\Psi_y|\right)/2$ and harmonic oscillation at frequency 2ω with an amplitude

$$\Psi_2 = \left(|\Psi_\theta| - |\Psi_y|\right)/2\,. \tag{24}$$

Substituting formulas (4), (6), (14), (15) into expressions (23) and calculating the integrals, we get the extremum values

$$\Psi_\theta = -\mu_0 \frac{\sin\theta_M \cos^2\theta_M}{8Mw_e^2} \frac{2k_\theta t_f + \sin(2k_\theta t_f)}{k_\theta \cos^2\left(k_\theta t_f\right)} \left(\mu_\theta - 1\right)^2 I_1^2,$$

$$\Psi_y = -\mu_0 \frac{\sin\theta_M \cos^2\theta_M}{8Mw_e^2} \frac{2k_\theta t_f + \sin(2k_\theta t_f)}{k_\theta \cos^2\left(k_\theta t_f\right)} \frac{\mu_{y\theta}^2}{\mu_{yy}^2} I_1^2. \tag{25}$$

From formulas (24) and (25) we find an oscillation amplitude of linear density of the magnetic induction flux at the doubled frequency between the strip conductor and the ground plane

$$\Psi_2 = \mu_0 \frac{t_f \sin\theta_M \cos^2\theta_M}{8Mw_e^2} \left| \frac{1 + \mathrm{sinc}(2k_\theta t_f)}{\cos^2\left(k_\theta t_f\right)} \right| \left(\left| \frac{\mu_{y\theta}^2}{\mu_{yy}^2} \right| - \left|\mu_\theta - 1\right|^2 \right) I_1^2\,. \tag{26}$$

To find current I_2 and voltage U_2 in MTL with a magnetic film at frequency 2ω, let us turn again to the system of telegraph equations taking into account the extraneous electromotive force from flux Ψ_2

$$\frac{\partial}{\partial z}U_2 + L(2\omega)\frac{\partial}{\partial t}I_2 = -\frac{\partial}{\partial t}\Psi_2, \quad \frac{\partial}{\partial z}I_2 + C\frac{\partial}{\partial t}U_2 = 0\,. \tag{27}$$

These equations can also be represented in a different form

$$\left(\frac{\partial^2}{\partial z^2} + k_2^2\right) I_2 = -\frac{k_2^2}{L(2\omega)}\Psi_2, \quad U_2 = -i\frac{Z_2}{k_2}\frac{\partial}{\partial z} I_2, \tag{28}$$

wave vector k_2 and characteristic impedance Z_2 in MTL at frequency 2ω assume values

$$k_2 = \frac{2\omega}{\tilde{n}}\sqrt{\varepsilon_e \mu_e(2\omega)}, \quad Z_2 = Z_0 \frac{t_g}{w_e}\sqrt{\mu_e(2\omega)/\varepsilon_e}\,. \tag{29}$$

The system of equations (28) after substituting formulas (20) and (26) into it assumes the final form

$$\left[\partial^2/\partial z^2 + k_2^2\right] I_2(z) = G k_2^2 I_1^2 \left[1+\cos(2k_1 z)\right], \quad U_2(z) = -iZ_2 k_2^{-1}\,\partial I_2/\partial z\,, \tag{30}$$

where nonlinearity factor G is determined by formula

$$G = \mu_0 \frac{t_\mathrm{f}\sin\theta_M \cos^2\theta_M}{16Mw_e^2 L(2\omega)} \left|\frac{1+\mathrm{sinc}(2k_\theta t_f)}{\cos^2\left(k_\theta t_f\right)}\right| \left(\left|\mu_\theta - 1\right|^2 - \left|\frac{\mu_{y\theta}^2}{\mu_{yy}^2}\right|\right). \tag{31}$$

Solution to the system of differential equations (30) has the form

$$\begin{gathered} I_2(z) = G I_1^2 \left[1 + \frac{k_2^2 \cos(2k_1 z)}{k_2^2 - 4k_1^2}\right] + X\cos(k_2 z), \\ U_2(z) = iZ_2\left[G I_1^2 \frac{2k_1 k_2 \sin(2k_1 z)}{k_2^2 - 4k_1^2} + X\sin(k_2 z)\right]. \end{gathered} \tag{32}$$

Here X is the undetermined constant that is to be determined when calculating the distribution of microwave field over all five segments of the resonator frequency multiplier.

Calculation of the examined microstrip structure will be performed within the one-dimensional model, in which only fundamental modes are considered. One can find the detailed description of such a calculation in [21]. There, the authors used this method to study the model of magnetic field sensor on a microstrip resonator with TMF. The frequency characteristics of the multiplier model were calculated in two stages.

At the first calculation stage, the system of non-uniform linear algebraic equations is solved. These equations are produced from Kirchhoff's laws at frequency ω for all nodes of the computational model, including its two ports. The amplitudes of waves on all irregular resonator segments at frequency ω are calculated based on the given amplitude of the wave incident on the input port. Among others, the amplitude of current I_1 in the grounding point is calculated. Calculation is performed in the linear approximation in relation to the amplitude of an incident wave. This means that we neglect the impact of weak oscillations excited at frequency 2ω.

At the second stage, current $I_2(z)$ and voltage $U_2(z)$ at frequency 2ω are calculated on the segment with magnetic film using formula (26). The value of current I_1 in point $z = 0$ produced during the first stage is used here. Then the system of non-uniform linear algebraic equations produced from Kirchhoff's laws for all nodal points at frequency 2ω is solved, and the value of current amplitude $I_{2\mathrm{out}}$ in the output port is found. The useful signal power at the doubled frequency is determined by expression $P_2 = Z_\mathrm{out} I_{2\,\mathrm{out}}^2/2$, where Z_out is the characteristic impedance of the output port.

2. RESEARCH RESULTS

Relying on the expressions produced above, we calculated the main characteristics of the examined frequency multiplier based on the microstrip resonator with TMF. It was assumed that the right part of the microstrip structure was made on high-Q ceramic substrate with permittivity $\varepsilon_d = 80$ and width $t_d = 0.5$ mm. For the sake of certainty, parameters of the device model were set in such a way that frequency of the first resonance $f_1 = \omega_1/2\pi$ was equal to 1 GHz, and frequency of the second resonance f_2 was equal to the doubled frequency of the first (2 GHz). The following geometric parameters of the line segments corresponded to these frequencies: width and length of the first segment $w_1 = 0.7$ mm, $l_1 = 1.9$ mm, the second – $w_2 = w_1$, $l_2 = 0.45$ mm, the third – $w_3 = 4$ mm, $l_3 = 3.55$ mm, the fourth – $w_4 = 0.16$ mm, $l_4 = 2.2$ mm, and the fifth $w_5 = 2.2$ mm, $l_5 = 1.6$ mm. We determined the optimal values of coupling capacities on the

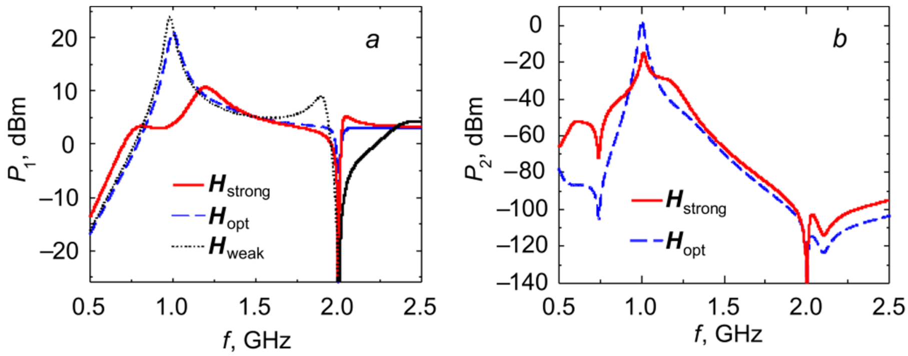

Fig. 4. Frequency dependences of the signal power on the output port calculated for three values of external field H_0: *a* – dependences of power P_1 at frequency f of input signal, *b* – dependences of power P_2 at doubled frequency $2f$.

input and output that are equal to $C_1 = 1.3$ pF and $C_2 = 1.8$ pF respectively. Characteristic impedances of the input and output ports $Z_{in} = Z_{out} = 50$ Ohm.

The input port for the signal on the first resonant frequency of the structure f_1 was conductively connected to conductor *4* (see Fig. 1) at the distance of 0.74 mm from its left end, which houses the node of the microwave electrical field for the second oscillation mode of the resonator that has the doubled resonant frequency $f_2 = 2f_1$. Such a connection prevents the useful signal (with the doubled frequency) from exiting through this port. For the efficient output of useful power, the output port of the structure is connected to strip conductor *3* (see Fig. 1) at the distance of 1.1 mm from the left end, where for the second oscillation mode of the resonator there is a high-frequency electrical field antinode that is the first from the grounded conductor end. It is important to note that connection of the output port close to the grounded end of the resonator conductor reduces the power losses of the input signal through this port, as far as electric field intensity for the first oscillation mode is small in this resonator region.

TMF made of permalloy ($Ni_{75}Fe_{25}$) was selected as a magnetic film. As one knows, such films, owing to their high permeability in the high-frequency range, are actively used in microwave equipment. The following parameters of the TMF sample were used in calculations: saturation magnetization $M = 1{\cdot}10^6$ A/m, anisotropy field $H_a = 550$ A/m, damping parameter $\alpha = 0.005$, conductivity $\sigma = 2.2{\cdot}10^6$ Ohm$^{-1}{\cdot}$m^{-1}, film thickness $t_f = 100$ nm. Easy magnetization axis was directed along MTL, i.e. had an angle $\theta_a = 0°$. It was assumed that the film was deposited onto the glass substrate ($\varepsilon_g = 10$) with thickness $t_g = 0.2$ mm. In all calculations, power of the input signal P was 0.5 W.

Properties of the resonator and primarily its loaded Q-factor depend on the value of external magnetic field H_0 applied to the magnetic film and the angle of its direction θ_H. To analyze the device operation, we selected three characteristic values of external field corresponding to variations in device operation: field $\boldsymbol{H}_{strong}$ ($H_0 = 400$ A/m, $\theta_H = 90°$) ensures the mode of strong TMF coupling with the resonator (the mode close to FMR), at which the film intensively absorbs electromagnetic energy, and Q-factor of the resonator is minimal; field $\boldsymbol{H}_{weak}$ ($H_0 = 1190$ A/m, $\theta_H = 0°$) corresponds to the weak coupling mode (far from FMR), at which magnetic film has almost no impact on the resonator; field $\boldsymbol{H}_{opt}$ ($H_0 = 1070$ A/m, $\theta_H = 80°$) implements the optimal coupling mode, at which the useful signal power at the doubled frequency becomes maximal.

Fig. 4*a* presents frequency dependences of the parasitic signal power P_1 registered on the output port at the same frequency f as the input signal frequency, and Fig. 4*b* presents frequency dependences of the useful signal power P_2 registered on the output port of the multiplier at the doubled frequency $2f$. Dependences are calculated for three values of external constant magnetic field $\boldsymbol{H}_{strong}$, $\boldsymbol{H}_{weak}$ and $\boldsymbol{H}_{opt}$ corresponding to three modes of film interaction with the resonator. As expected, in the mode of weak TMF coupling with the resonator, the second harmonic generation is not observed, because permeability of the film is equal to one.

In the strong coupling mode, when imaginary part of magnetic permeability μ_θ at the first resonant frequency is maximal, the film intensively absorbs the wave energy. Q-factor of the resonator goes down considerably, and the output power P_1 in this mode at the first resonant frequency is by approximately two orders of magnitude smaller than

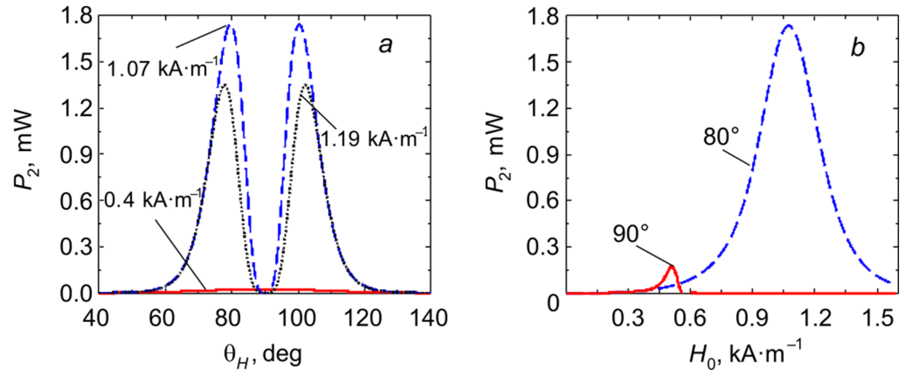

Fig. 5. Dependences of signal power P_2 at the doubled frequency: *a* – angular dependences $P_2(\theta_H)$ for three field values H_0, *b* – field dependences $P_2(H_0)$ for two angle values θ_H.

P_1 in the weak coupling mode. Linear induction of MTL with a thin film increases, which leads to significant displacement of eigen resonator frequencies. In the optimal coupling mode, signal generation at the doubled frequency $2f=f_2$ = 2 GHz is maximal and equals 2.4 dBm (1.74 mW). Output signal power P_1 at the first resonant frequency 1 GHz (Fig. 4*a*) occupies an intermediary position between values of P_1 calculated at this frequency for two other modes. Maximum second harmonic generation is observed, when only part of the wave energy in the resonator is absorbed by the film (~40% vs. ~99% in the strong coupling mode). It is important to note that the useful signal power P_2 obtained at optimal external field parameters is almost by two orders of magnitude larger than the power generated in the strong coupling mode. Therefore, at optimal parameters of external static magnetic field, conversion coefficient of the examined multiplier $K = 100\%\cdot P_2/P$, determined as the relationship of the signal power at the doubled frequency P_2 to the input power P and expressed in percentage points, is 0.35% at P = 500 mW and f = 1 GHz.

Fig. 5 presents the dependences of power P_2 at the doubled frequency on direction θ_H and value H_0 of external magnetic field at the input signal frequency $f = f_1$ = 1 GHz. For a fixed field value H_0 = 1.07 kA/m with angle increase θ_H, value P_2 first grows exponentially reaching the maximum at $\theta_H = 80°$ and then abruptly decreases to zero at $\theta_H = 90°$. The mirror symmetry observed on the dependence $P_2(\theta_H)$ in relation to $\theta_H = 90°$ is caused by uniaxial magnetic anisotropy of the film. It is interesting to note that when external magnetic field is directed along the hard magnetization axis, the signal at the doubled frequency is absent for most field values. And only at values approximately corresponding to the strong coupling mode, power P_2 is different from zero.

Dependence of the signal power at the doubled frequency on the external static field applied to a magnetic film is caused by several factors. First, external magnetic field can change orientation of the equilibrium magnetization vector of the film $\boldsymbol{M}_0$. In the examined multiplier, excitation and detection of magnetization oscillations is done by the same MTL segment located above the magnetic film. The oscillations are excited in the most efficient manner, when direction of the microwave field is orthogonal to $\boldsymbol{M}_0$, i.e. when equilibrium magnetization is oriented along MTL. At the same time, as far as oscillating magnetization at the doubled frequency is directed along vector $\boldsymbol{M}_0$, amplitude of the microwave current generated in the segment by "quadratic" magnetization is proportional to the projection of equilibrium magnetization onto axis x that is perpendicular to the MTL segment. Term $\sin\theta_M\cos^2\theta_M$ that is part of expression (26) and assumes the maximum at $\theta_M = 35°$ meets these two conditions. Let us note that in the optimal coupling mode, the equilibrium angle $\theta_M = 61°$, and in the strong coupling mode $\theta_M = 35°$.

The second factor that affects the second harmonic generation and depends on the external field is magnetic permeability of the film described by the second rank tensor $\ddot{\mu}/\mu_0$ (6). Different components of this tensor are part of expression (26) for the induction flux Ψ_2 that generates oscillations at the doubled frequency. However, the main contribution is made by value μ_θ (see formula (15)) that is the effective permeability for an electromagnetic wave, the magnetic field of which is directed orthogonally to equilibrium magnetization.

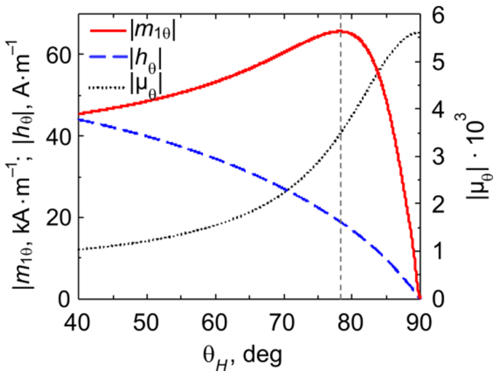

Fig. 6. Dependences of absolute values of effective permeability $|\mu_\theta|$, microwave field $|h_\theta|$ and oscillating magnetization $|m_{1\theta}|$ on direction of external field θ_H at its value $H_0 = 1.07$ kA/m and $f = 1$ GHz.

To clarify the effect of permeability μ_θ on the second harmonic generation, let us consider the dependence of its absolute value $|\mu_\theta|$ on the direction of external field θ_H at field value $H_0 = 1.07$ kA/m and $f = 1$ GHz (Fig. 6). One can see that as angle θ_H goes up, parameter $|\mu_\theta|$ gradually grows, reaching the maximum at $\theta_H = 90°$. The same graph presents an angular dependence of the absolute value of high-frequency field $|h_\theta|$ calculated in the film center ($y = -t_f/2$). One can see that field $|h_\theta|$ decreases with the increase in angle θ_H. As a result, these two dependences reflect the fact that value of the microwave magnetic field in the microstrip resonator decreases with the increase in magnetic permeability module of TMF, presumably due to absorption of the microwave power by the film that leads to the decrease in the loaded Q-factor of the resonator, and hence to the corresponding decrease in the energy stored up in it. Component of linear variable magnetization $m_{1\theta}$ is linked with microwave magnetic field by expression $m_{1\theta} = (\mu_\theta - 1)h_\theta$, that is why its maximum will be reached only at some optimal values of μ_θ and h_θ. In Fig. 6, the dashed vertical line $\theta_H = 78°$ marks the position of the maximum $|m_{1\theta}|$ observed at a relatively small amplitude of high-frequency field (19 A/m), but at magnetic permeability of TMF that is large in absolute terms ($3.4 \cdot 10^3$).

The need to search for balance between energy absorption and accumulation in the resonator, in order to achieve the maximum level of the second harmonic generation is well illustrated by topological graphs presented in Fig. 7. They show the dependences of the absolute value of nonlinearity factor $|G|$, absolute value of the microwave current amplitude $|I_1|$ on the segment of the quarter-wavelength resonator with TMF (see Fig. 1) and signal power at the doubled frequency P_2 on the value H_0 of external static magnetic field and its orientation θ_H. As before, frequency of the input signal in these calculations $f = f_1 = 1$ GHz. On all topologies, the + marks indicate the points, where the second harmonic generation is maximal. Nonlinearity factor G determined by expression (31) describes the nonlinear response of magnetic film. One can see that the optimum points lie on its slopes far from the maximum. At the same time, current $|I_1|$, on which component m_{2x} depends quadratically, assumes some intermediary value between the maximum and the minimum in the optimum point. Behavior of these two values provides explanation for the type of dependence of power P_2 on magnetic field parameters, since $P_2 \sim GI_1^2$.

CONCLUSIONS

Therefore, the present paper suggests and theoretically examines the resonator design of the frequency doubler. The nonlinear element of the multiplier is a thin magnetic film deposited onto the glass substrate. The film is located in the MTL segment of the irregular quarter-wavelength resonator consisting of five regular segments. One end of the MTL segment is grounded. Owing to the selected width and length of strip conductors of regular MTL segments, such a resonator, unlike the regular quarter-wavelength resonator, has not the tripled, but the doubled resonant frequency of the second oscillation mode. Furthermore, resonant frequencies of its higher oscillation modes are not multiples of the first mode frequency, which significantly reduces the losses of microwave power to the higher harmonics. Another

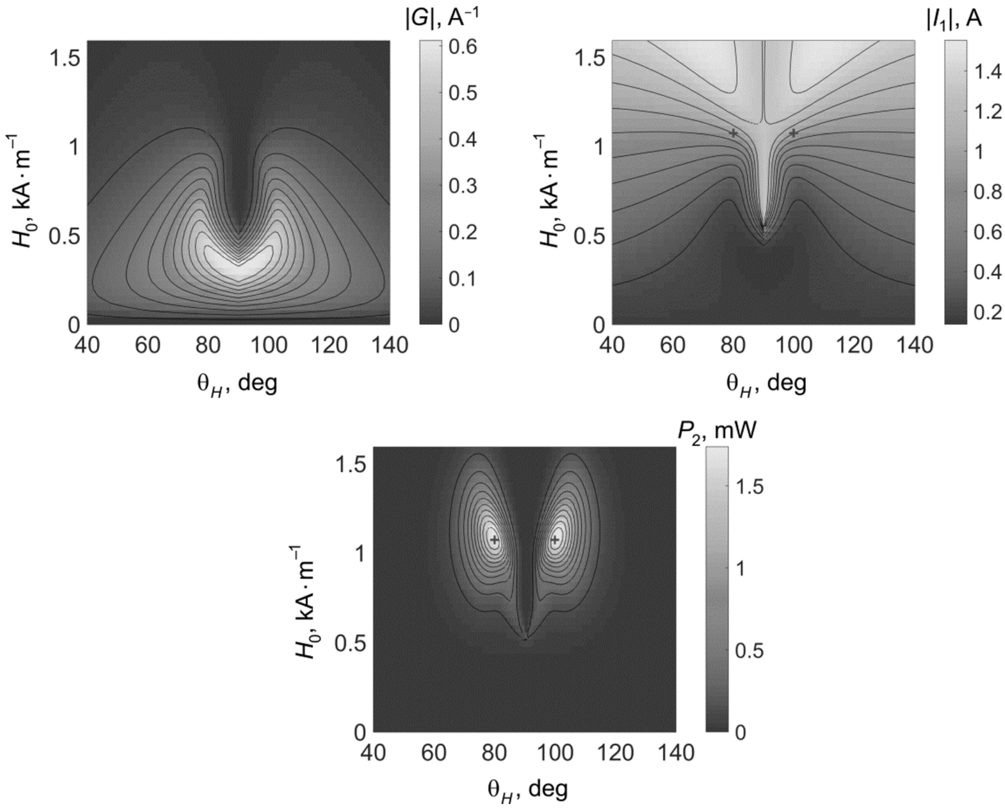

Fig. 7. Distributions in space (θ_H, H_0) of the absolute value of nonlinearity factor $|G|$, current $|I_1|$ at frequency $f = f_1$ = 1 GHz and signal power P_2 at the doubled frequency $2f$.

important feature of the examined layout is the connection of the input port to the strip conductor of the resonator to the point, where the node of high-frequency electric field for the second oscillation mode is located, which prevents the useful signal with the doubled frequency from exiting through this port.

Propagation and nonlinear interaction of the fundamental modes in MTL containing a ferromagnetic film were calculated in the quasi-static approximation by solving the telegraph equations. Calculations of linear capacities and inductances of MTL were performed within the Oliner model by replacing the microstrip line with an equivalent flat waveguide with corresponding MTL parameters. Quadratic magnetization response was determined from the solution to the Landau-Lifshitz equation. The calculation took into account both magnetic and ohmic loss in the film.

It was shown that depending on direction and strength of external static magnetic field, there is a change in the degree of film impact on the frequency response of the resonator. This is due to the fact that under the impact of magnetic field there is a change in orientation of equilibrium magnetization and magnetic permeability of the film. It was established that the second harmonic generation is maximal at optimal values of the magnitude and direction of external magnetic field, when a certain balance is reached between absorption and accumulation of energy in the resonator. Conversion coefficient of the multiplier in this case is 0.35% at the input signal power of 500 mW at the resonant frequency of the structure of 1 GHz. Let us note that the produced behavioral regularities of the useful signal power in the frequency multiplier associated with the direction and strength of external magnetic field are very important when creating and optimizing such devices.

This research was carried out with financial support of the Ministry of Science and Higher Education of the Russian Federation, agreement number 075-11-2019-054 dated 22.11.2019, and the Russian Science Foundation within the research project No. 19-72-10047.

REFERENCES

1. V. K. Arkadiev, Journal of the Russian Physics and Chemistry Society, physics section [in Russian], **44**, 165–200 (1912).
2. D. Jaffe, J. C. Cacheris, and N. Karayianis, Proc. IRE., **46**, 594–601 (1958).
3. E. N. Skomal and M. A. Medina, J. Appl. Phys., **29**, 423–424 (1958).
4. W. P. Ayres, P. H. Vartanian, and J. L. Melchor, J. Appl. Phys., **27**, 188–189 (1956).
5. A. S. Risley and I. Kaufman, J. Appl. Phys., **33**, 1269 (1962).
6. I. Bady, IEEE Trans. Microwave Theory Tech., **10**, 55–64 (1962).
7. J. L. Melchor, W. P. Ayres, and P. H. Vartanian, Proc. IRE., **45**, 643–646 (1957).
8. E. Schied and O. Weis, JMMM, **45**, 377–381 (1984).
9. J. Petzold, JMMM, **242–245**, 84–89 (2002).
10. M. Yamaguchi, K. Hyeon Kim, and S. Ikedaa, JMMM, **304**, 208–213 (2006).
11. B. A. Belyaev, A. V. Izotov, P. N. Solovev, and N. M. Boev, Phys. Status Solidi RRL – Rapid Res. Lett., **14**, 1900467 (2020).
12. P. N. Solovev, A. V. Izotov, and B. A. Belyaev, JMMM, **429**, 45–51 (2017).
13. B. A. Belyaev, A. V. Izotov, and P. N. Solovev, Phys. B. Condens. Matter., **481**, 86–90 (2016).
14. J. Marsh, V. Zagorodnii, Z. Celinski, and R. E. Camley, Appl. Phys. Lett., **100**, 102404 (2012).
15. C. Cheng and W. E. Bailey, Appl. Phys. Lett., **103**, 242402 (2013).
16. Y. Khivintsev, J. Marsh, V. Zagorodnii, *et al.*, Appl. Phys. Lett., **98**, 042505 (2011).
17. M. Bao, A. Khitun, Y. Wu, *et al.*, Appl. Phys. Lett., **93**, 072509 (2008).
18. B. A. Belyaev, A. V. Izotov, S. Ya. Kiparisov, G. V. Skomorokhov, J. Phys. of the Solid State, **50**, Issue 4, 676–683 (2008).
19. A. A. Oliner, IEEE Trans. Microwave Theory Tech., **3**, 134–143 (1955).
20. A. G. Gurevich, G. A. Melkov, Magnetic Oscillations and Waves [in Russian], Nauka, Moscow (1994).
21. B. A. Belyaev, N. M. Boev, A. V. Izotov, *et al.*, Russ. Phys. J., **61**, Issue 8, 1367–1375 (2018).